

# ***D*-wave electron-H, -He<sup>+</sup>, and -Li<sup>2+</sup> elastic scattering and photoabsorption in *P* states of two-electron systems**

A. K. Bhatia

*Heliophysics Science Division, NASA/Goddard Space Flight Center, Greenbelt, Maryland 20771, USA*

(Received 17 April 2014; published 30 June 2014)

In previous papers [A. K. Bhatia, *Phys. Rev. A* **85**, 052708 (2012); **86**, 032709 (2012); **87**, 042705 (2013)] electron-H, -He<sup>+</sup>, and -Li<sup>2+</sup> *P*-wave scattering phase shifts were calculated using the variational polarized orbital theory. This method is now extended to the singlet and triplet *D*-wave scattering in the elastic region. The long-range correlations are included in the Schrödinger equation by using the method of polarized orbitals *variationally*. Phase shifts are compared to those obtained by other methods. The present calculation provides results which are rigorous lower bounds to the exact phase shifts. Using the presently calculated *D*-wave and previously calculated *S*-wave continuum functions, photoionization of singlet and triplet *P* states of He and Li<sup>+</sup> are also calculated, along with the radiative recombination rate coefficients at various electron temperatures.

DOI: 10.1103/PhysRevA.89.062720

PACS number(s): 34.80.Bm

## I. INTRODUCTION AND CALCULATIONS

Collision between an electron and the target is a many-body problem. The perturbation in the target due to the incident electron induces in it electric multipole moments. The exact knowledge of the single-electron targets makes it possible to obtain accurate results. In general, it is not possible to infer phase shifts, resonance parameters, photoabsorption cross sections, radiative-attachment rates, and cross sections for free-free absorption of radiation by scaling as the nuclear charge is increased. Phase shifts are also required in the calculations of laser-assisted free-free transitions in electron-atom collisions [1,2]. Therefore, it becomes important to carry out calculations in each case.

At low energies, in addition to the exchange between the electrons, the distortion of the target produced by the incident electrons is important. This distortion can be taken into account by the method of polarized orbitals [3,4] which includes the effect of polarization in the ansatz of the wave function of the target. Other approximations for calculating phase shifts are the Kohn-Feshbach variational method [5], the Kohn variational method [6], the *R*-matrix method [7], and the finite element method [8]. The electron-hydrogenic systems *D*-wave phase shifts in the elastic region have been calculated by Sloan [9] and by Khan *et al.* [10] using the method of polarized orbitals and by Gien [11,12] using the Harris-Nesbet method. The electron-H, -He<sup>+</sup>, and -Li<sup>2+</sup> *S*-wave and *P*-wave phase shifts in the elastic region have been calculated [13–17] in which the long-range potential proportional to  $-1/r^4$  was included *variationally*.

It is well known that the photodetachment of H<sup>-</sup> contributes to the opacity of the sun. Similarly, photoionization and its reverse process, radiative recombination, in atoms and ions are needed in the solar and in the stellar modeling of the opacity. Since the excited states have lower threshold energies for ionization, much less photon energy is required for photoionization. These photoelectrons then excite various levels of the plasma constituents which decay to the lower levels, providing spectra of various astrophysical objects for diagnostic purposes. The observations of such spectra help to infer the electron densities, temperatures, and element abundances of the astrophysical plasmas. We use Rydberg

units: energy in Rydbergs, length in Bohr radius  $a_0$ , and phase shifts in radians.

We briefly describe the formalism already discussed in previous papers on *S* and *P* scattering states. In order to obtain the Schrödinger equation, the total spatial wave function for the electron-target partial wave (denoted by *L*) problem is written as

$$\Psi_L(\vec{r}_1, \vec{r}_2) = \frac{u(r_1)}{r_1} Y_{L0}(\hat{r}_1) \Phi^{\text{pol}}(r_1, r_2) \pm (1 \leftrightarrow 2). \quad (1)$$

The ( $\pm$ ) above refers to singlet (upper sign) or triplet (lower sign) scattering, respectively. The effective target wave function can be written as

$$\Phi^{\text{pol}}(\vec{r}_1, \vec{r}_2) = \phi_0(\vec{r}_2) - \frac{\chi_\beta(r_1)}{r_1^2} \frac{u_{1s \rightarrow p}(r_2)}{r_2} \frac{\cos(\theta_{12})}{\sqrt{Z\pi}}, \quad (2)$$

where

$$\phi_0(\vec{r}_2) = \sqrt{\frac{Z^3}{\pi}} e^{-Zr_2}, \quad (3)$$

$$u_{1s \rightarrow p}(r_2) = e^{-Zr_2} \left( \frac{Z}{2} r_2^3 + r_2^2 \right), \quad (4)$$

and  $\theta_{12}$  is the angle between  $\vec{r}_1$  and  $\vec{r}_2$ . We have replaced the step function  $\varepsilon(r_1, r_2)$ , used by Temkin [4], by a smooth cutoff function  $\chi_\beta(r_1)$  which is of the form

$$\chi_\beta(r_1) = (1 - e^{-\beta r_1})^n, \quad (5)$$

where  $n \geq 3$ . Now the polarization of the target takes place whether the scattered electron is inside or outside the orbital electron. The polarization function given in Eq. (2) is valid throughout the range. This is unlike the step function  $\varepsilon(r_1, r_2)$  used in [4] which ensures that the polarization takes place when the scattered electron  $r_1$  is outside the orbital electron  $r_2$ . Furthermore, the function in Eq. (5) gives us another parameter,  $\beta$ , which is a function of  $k$ , the incident electron momentum. This term guarantees that  $\chi_\beta(r_1)/r_1^2 \rightarrow 0$  when  $r_1 \rightarrow 0$  and it also contributes to the short-range correlations, and therefore is useful to optimize the results.

Beyond the terms containing  $u(r)$  explicitly, are the terms giving rise to the exchange approximation, here  $L = 2$ . The

TABLE I. Comparison of phase shift  $\eta$  (radians) for  $e$ -H scattering with those obtained with the method of polarized orbitals [4].

$k$	$^3D$		$^1D$	
	Present $\eta$	$\eta_{PO}$ [4]	Present $\eta$	$\eta_{PO}$ [4]
0.1	1.3217(-3)		1.3193(-3)	
0.2	5.0835(-3)		5.0217(-3)	
0.3	1.0898(-2)	1.18(-2)	1.0531(-2)	1.13(-2)
0.4	1.8401(-2)		1.7250(-2)	
0.5	2.7204(-2)		2.4675(-2)	2.66(-2)
0.6	3.6934(-2)		3.2495(-2)	
0.7	4.7286(-2)		4.0544(-2)	
0.75	5.2614(-2)	7.46(-2)	4.4596(-2)	4.56(-2)
0.8	5.7990(-2)		4.8620(-2)	
0.9	6.8791(-2)		5.6532(-2)	
1.0	7.9484(-2)	1.12(-1)	6.4024(-2)	6.27(-2)

scattering function  $u(r)$  is obtained by solving the integrodifferential equations resulting from

$$\int [Y_{20}^*(\Omega_1)\Phi^{\text{pol}}(\vec{r}_1, \vec{r}_2)(H - E)\Psi_L]d\vec{r}_2 = 0. \quad (6)$$

In the above equation  $H$  is the Hamiltonian and  $E$  is the total energy of the electron-target scattering system:

$$H = -\nabla_1^2 - \nabla_2^2 - \frac{2Z}{r_1} - \frac{2Z}{r_2} + \frac{2}{r_{12}}, \quad (7)$$

$$E = k^2 - Z^2. \quad (8)$$

$k^2$  is the kinetic energy of the incident electron and  $Z$  is the nuclear charge. The integrodifferential equations are solved by the noniterative method [18]. The phase shifts are inferred by knowing the scattering function at  $r \equiv r_1 \rightarrow \infty$ ,

$$\lim_{r \rightarrow \infty} u(r) \propto \sin \left[ kr + \frac{l(l+1)}{r^2} + \frac{Z-1}{k} \ln(2kr) + \arg \Gamma \left( 1 - \frac{i(Z-1)}{k} \right) + \eta \right]. \quad (9)$$

The phase shifts for  $^3D$  and  $^1D$  scattering states for  $e$ -H, given in Table I, are compared with those obtained in [4] using the method of polarized orbitals. The present results for both triplet and singlet states are lower than those obtained in [4], except for  $k > 0.8$ , where they are higher in the singlet state. The results in [4] have no variational bounds, while the present results have variational lower bounds. Similar results for  $^3D$  and  $^1D$  scattering states have been obtained for  $e$ -He $^+$ . They are given in Table II and compared with those obtained by Sloan [9] using the method of polarized orbitals. The present results for triplet states are lower, while for singlet states they are higher than those obtained in [9]. Khan *et al.* [10], taking into account the exchange-polarization terms also, have carried out calculations similar to those of Sloan and their results for both states are lower than those of [9]. However, the results in [9,10] are not in agreement with the present variational calculations, which are expected to be accurate because of the bound on the phase shifts.

TABLE II. Comparison of phase shift  $\eta$  (radians) for  $e$ -He $^+$  scattering with those obtained with the method of polarized orbitals [9].

$k$	$^3D$		$^1D$	
	Present $\eta$	$\eta_{PO}$ [9]	Present $\eta$	$\eta_{PO}$ [9]
0.1	8.5133(-3)		5.9268(-3)	
0.2	9.0331(-3)	1.06(-2)	6.1299(-3)	6.40(-3)
0.3	9.8834(-3)		6.4446(-3)	
0.4	1.1044(-2)	1.33(-2)	6.8511(-3)	7.10(-3)
0.5	1.2473(-2)		7.3028(-3)	
0.6	1.4152(-2)	1.74(-2)	7.7904(-3)	8.0(-3)
0.7	1.6066(-2)		8.3087(-3)	
0.8	1.8172(-2)	2.27(-2)	8.8420(-3)	8.8(-3)
0.9	2.0439(-2)		9.3860(-3)	
1.0	2.2841(-2)	2.87(-2)	9.9534(-3)	9.5(-3)
1.1	2.5346(-2)		1.0547(-2)	
1.2	2.7921(-2)	3.51(-2)	1.1173(-2)	1.03(-2)
1.3	3.0549(-2)		1.1851(-2)	
1.4	3.3233(-2)	4.26(-2)	1.2631(-2)	
1.5	3.5939(-2)		1.3454(-2)	
1.6	3.8573(-2)	4.77(-2)	1.4306(-2)	1.26(-2)
1.7	4.1158(-2)		1.5206(-2)	
1.8	4.3673(-2)		1.6152(-2)	
1.9	4.6125(-2)		1.7135(-2)	
2.0	4.8454(-2)		1.8149(-2)	1.66(-2)

Phase shifts for  $^3D$  and  $^1D$  scattering states have also been calculated for  $e$ -Li $^{2+}$ . They are given in Table III and compared with those obtained in [10] using the method of polarized orbitals. Again, the present results for triplet states are lower,

TABLE III. Comparison of phase shift  $\eta$  (radians) for  $e$ -Li $^{2+}$  scattering with those obtained with the method of polarized orbitals [10].

$k$	$^3D$		$^1D$	
	Present $\eta$	$\eta_{PO}$ [10]	Present $\eta$	$\eta_{PO}$ [10]
0.1	8.2703(-3)		3.0363(-3)	
0.2	8.4642(-3)		3.0585(-3)	
0.3	8.7011(-3)		3.0508(-3)	
0.4	9.0700(-3)	1.00(-2)	3.0776(-3)	2.58(-3)
0.5	9.5041(-3)	1.06(-2)	3.0782(-3)	2.54(-3)
0.6	1.0009(-2)	1.13(-2)	3.0608(-3)	2.50(-3)
0.7	1.0622(-2)	1.21(-2)	3.0831(-3)	2.46(-3)
0.8	1.1380(-2)	1.30(-2)	3.1396(-3)	2.41(-3)
0.9	1.2151(-2)	1.39(-2)	3.1537(-3)	2.37(-3)
1.0	1.2984(-2)	1.50(-2)	3.1657(-3)	2.32(-3)
1.1	1.3868(-2)	1.61(-2)	3.1730(-3)	2.27(-3)
1.2	1.4790(-2)	1.73(-2)	3.1723(-3)	2.23(-3)
1.3	1.5735(-2)	1.85(-2)	3.1575(-3)	2.20(-3)
1.4	1.6689(-2)	1.97(-2)	3.1257(-3)	2.17(-3)
1.5	1.7770(-2)	2.10(-2)	3.2378(-3)	2.16(-3)
1.6	1.8623(-2)	2.23(-2)	3.5411(-3)	2.16(-3)
1.7	1.9782(-2)	2.36(-2)	3.6550(-3)	2.18(-3)
1.8	2.0921(-2)	2.48(-2)	3.7901(-3)	2.21(-3)
1.9	2.2067(-2)	2.61(-2)	3.9474(-3)	2.27(-3)
2.0	2.3214(-2)	2.73(-2)	4.1272(-3)	2.35(-3)

TABLE IV. Total elastic scattering and the spin-flip cross sections for  $e$ -H in units of  $a_0^2$ .  $S$ -wave phase shifts are from [13],  $P$ -wave phase shifts are from [15], and  $D$ -wave phase shifts are the present results given in Table I.

$k$	$\sigma(l=0)^a$	$\sigma(l=0) + \sigma(l=1)^b$	$\sigma(l=0) + \sigma(l=1)$		$\sigma_{\text{SF}}$
				$+ \sigma(l=2)^c$	
0.1	134.9527	135.0669	135.3064		44.2952
0.2	100.6217	101.1241	102.1693		29.0073
0.3	71.8754	73.0780	75.5647		18.9188
0.4	52.2387	54.3175	58.6040		13.5072
0.5	38.8344	41.5355	47.1154		10.4705
0.6	29.3916	32.3317	38.4364		8.3908
0.7	22.5298	25.3547	31.2720		6.6208
0.8	16.6011	20.1350	25.5083		4.9005

<sup>a</sup>Obtained by using  $S$ -wave phase shifts only.

<sup>b</sup>Obtained by using  $S$ - and  $P$ -wave phase shifts.

<sup>c</sup>Obtained by using  $S$ -,  $P$ -, and  $D$ -wave phase shifts.

while for singlet states they are higher than those obtained in [10].

Phase shifts for  $L = 0, 1$ , and  $2$  for  $e$ -H scattering are used to calculate total cross sections at various incident energies. The theoretical results are useful because, in general, it is difficult to measure cross sections in the forward direction.

The total cross section is given by

$$\sigma = 0.25\sigma_S + 0.75\sigma_T, \quad (10)$$

where

$$\sigma_S = \frac{4\pi}{k^2} \sum_l (2l+1) \sin^2(\eta_S) \quad (11)$$

and

$$\sigma_T = \frac{4\pi}{k^2} \sum_l (2l+1) \sin^2(\eta_T). \quad (12)$$

In the above equation  $\eta_S$  and  $\eta_T$  are the singlet and triplet phase shifts, respectively. The spin-flip cross section is given by

$$\sigma_{\text{SF}} = \frac{\pi}{k^2} \sum_l (2l+1) \sin^2(\eta_S - \eta_T). \quad (13)$$

The results for  $\sigma$  and  $\sigma_{\text{SF}}$  are given for electron-hydrogen scattering in Table IV for various incident electron momenta. The  $S$ -wave and  $P$ -wave phase shifts are very accurate as they have been obtained by using the hybrid theory, while the  $D$ -wave phase shifts are obtained here in the variational polarized approximation and they are small relative to the  $S$ -wave and  $P$ -wave results. The cross sections given in Table IV are expected to be fairly accurate. In this table, the convergence of the elastic cross section is shown as the contributions from  $S$ ,  $P$ , and  $D$  partial waves are added.

## II. PHOTOIONIZATION OF EXCITED $P$ STATES IN He AND Li<sup>+</sup>

Photoionization processes are important in the study of the upper atmosphere physics and for stellar modeling. The dominant processes determining the ionization structure of any plasma are photoionization (in addition to collisional

ionization) and its inverse process, radiative recombination. In a previous paper [17], we calculated the photoabsorption cross sections of  $S$  states of two-electron systems: H<sup>-</sup>, He, and Li<sup>+</sup>. In this process, the final continuum state of the photoelectron is the  $P$  state when the target is left in the ion ground state. It is known that the opacity in the sun is due to the photodetachment of H<sup>-</sup>. In the photoionization of the  $P$  states, the final continuum states of the photoelectron are  $S(l_f = 0)$  and  $D(l_f = 2)$  states. Both these final states must be included in the calculation of the total photoabsorption cross section. The general expression for the cross section at low photon energies (below 1000 eV) is given in the dipole approximation by

$$\sigma(l_f) = \frac{4\pi(2l_f + 1)\alpha k\omega}{3(2l_i + 1)} \left| \langle \Psi_{l_f} | z_1 + z_2 | \Phi_i \rangle \right|^2, \quad (14)$$

where  $\alpha$  is the fine-structure constant,  $\Phi_i$  is the initial bound  $P$ -state wave function with  $l_i = 1$ ,  $\Psi_{l_f}$  is the final continuum wave function of the outgoing electron with the momentum  $k$ , and  $\omega$  is the energy of the incident photon:

$$\omega = I + k^2. \quad (15)$$

$I$  is the ionization potential of the system absorbing the photon, and  $k^2$  is the energy of the photoelectron, and they are in Rydberg units. Therefore, the total cross section is given by

$$\sigma = \sigma(l_f = 0) + \sigma(l_f = 2). \quad (16)$$

Here we use the length form for the cross section because this form is most suitable when the long-range correlations are included in the final-state wave functions and most of the contributions to the matrix elements in Eq. (10) come from the outer region rather than the region close to the nucleus.  $\Psi_S$  and  $\Psi_D$ , the continuum  $S$  and  $D$  states of the photoelectron, have the form given in Eq. (1). We assume in the derivation of Eq. (14), the plane-wave normalization. Therefore, we have the coefficient  $4\pi(2l_f + 1)$  in Eq. (14).  $\Phi_i$ , the  $^{1,3}P$ -state wave function of the target, is of the Hylleraas form and is given by

$$\Phi_i(\vec{r}_1, \vec{r}_2) = [f_1^{+1}(r_1, r_2, r_{12})D_1^{+1}(\theta, \phi, \psi) + f_1^{-1}(r_1, r_2, r_{12})D_1^{-1}(\theta, \phi, \psi)]. \quad (17)$$

The  $D_1^\varepsilon$  functions ( $\varepsilon = +1, -1$ ) are called *rotational harmonics* [19]. The  $f$ 's are the generalized "radial" functions, which depend on the three residual coordinates that are required (beyond the Euler angles) to define two vectors,  $\mathbf{r}_1$  and  $\mathbf{r}_2$ . The distance between the two electrons is given by  $r_{12} = |\mathbf{r}_1 - \mathbf{r}_2|$ . The radial functions  $f_1^{\pm 1}$  are defined as follows:

$$f_1^{+1} = \cos(\theta_{12}/2)[f(r_1, r_2, r_{12}) \pm f(r_2, r_2, r_{12})], \quad (18)$$

$$f_1^{-1} = \sin(\theta_{12}/2)[f(r_1, r_2, r_{12}) \mp f(r_2, r_2, r_{12})], \quad (19)$$

and

$$f(r_1, r_2, r_{12}) = e^{-ar_1 - br_2} \sum_{lmn} D_{lmn} r_1^l r_2^m r_{12}^n. \quad (20)$$

The upper sign in Eqs. (18) and (19) refers to the singlet state and the lower sign refers to the triplet state. The minimum value of  $l = 1$  in Eq. (20), while the minimum values of  $m$  and  $n$  are 0. The nonlinear parameters are  $a$  and  $b$ , and  $D_{lmn}$  are the eigenvectors. Energies for various numbers of terms are given in Table XIII in the Appendix for the He

TABLE V. Convergence of photoionization cross sections (Mb) for the  $^3P$  excited states, outgoing electron in  $L = 0$ .

$k$	System, state	$N_\omega = 220$	286	364
0.1	He, $(1s3p)^1P$	2.3792(-1)	2.3897(-1)	2.3910(-1)
0.2		1.7971(-1)	1.8014(-1)	1.8014(-1)
0.3		1.1729(-1)	1.1704(-1)	1.1695(-1)
0.1	He, $(1s3p)^3P$	7.9846(-1)	7.9618(-1)	7.9048(-1)
0.2		4.7052(-1)	4.7263(-1)	4.6521(-1)
0.3		2.2888(-1)	2.3005(-1)	2.3191(-1)
0.1	He, $(1s4p)^3P$	1.2989	1.4004	1.3997
0.2		6.6288(-1)	6.1820(-1)	6.0959(-1)
0.3		2.3623(-1)	2.1905(-1)	2.2155(-1)
0.1	Li <sup>+</sup> , $(1s2p)^3P$	6.2094(-1)	5.9150(-1)	5.9179(-1)
0.2		5.7604(-1)	5.4871(-1)	5.4893(-1)
0.5		3.4065(-2)	3.2401(-2)	3.2391(-2)
0.1	He, $(1s2p)^1P$	2.6767(-1)	2.6942(-1)	2.6918(-1)
0.2		2.0524(-1)	2.0524(-1)	2.0605(-1)
0.3		1.3887(-1)	1.3835(-1)	1.3860(-1)
0.1	He, $(1s3p)^1P$	7.2160(-1)	7.3152(-1)	7.3841(-1)
0.2		4.3695(-1)	4.3692(-1)	4.3019(-1)
0.3		2.1792(-1)	2.1427(-1)	2.1182(-1)
0.1	He, $(1s4p)^1P$	1.1961	1.2607	1.2628
0.2		5.8137(-1)	5.6109(-1)	5.3909(-1)
0.3		2.0384(-1)	1.9402(-1)	2.0020(-1)
0.1	Li <sup>+</sup> , $(1s2p)^1P$	5.5857(-2)	5.5979(-2)	5.6034(-2)
0.2		5.1967(-2)	5.2093(-2)	5.2144(-2)
0.3		4.6322(-2)	4.6440(-2)	4.6482(-2)
0.1	Li <sup>+</sup> , $(1s3p)^1P$	1.7283(-1)	1.7287(-1)	1.7369(-1)
0.2		1.4949(-1)	1.4966(-1)	1.5008(-1)
1.3		3.0617(-3)	3.0682(-3)	3.0363(-3)

atom and the Li<sup>+</sup> ion. The cross section has a finite value for  $k \rightarrow 0$  which is due to the fact that the final-state function is a Coulomb function, therefore  $u(r) \propto 1/\sqrt{k}$ , and the expression for the cross section becomes independent of  $k$ , the outgoing photoelectron momentum. It is known that there are no bound excited states of H<sup>-</sup> ions, therefore no photodetachment cross sections have been calculated for the excited  $P$  states.

In Table V, we show the convergence of the photoionization cross sections for a few values of the outgoing electron momentum  $k$  for the  $(1s2p)$ ,  $(1s3p)$ , and  $(1s4p)^{1,3}P$  states of He and Li<sup>+</sup>, when the outgoing electron is in the  $S$  continuum state. The convergence with respect to the number of terms  $N_\omega = 220, 286,$  and  $364$  in the  $P$  state shows that the cross sections have converged in the third or fourth decimal place in most cases. The cross sections decrease as  $k$  increases and are seen to be larger for the higher excited states.

In Table VI, we give the photoabsorption cross sections, when the outgoing photoelectron is in the continuum  $D$  state, for various excited states in He and Li<sup>+</sup>. It is seen that these cross sections are much larger than the cross sections when the continuum electron is in the  $S$  state. They also decrease as  $k$  increases and are larger for the higher excited states.

In Table VII, partial and total cross sections  $\sigma$  [Eq. (16)] for  $^3P$  states of He are given for various outgoing photoelectron momenta, and in Table VIII similar results for  $^1P$  states of He are given. In general, triplet state photoionization cross sections are larger than the singlet ones. Also, the cross sections

TABLE VI. Convergence of photoionization cross sections (Mb) for the  $^3P$  excited states,  $L = 2$ .

$k$	System, state	$N_\omega = 220$	286	364
0.1	He, $(1s2p)^3P$	21.0188	21.0511	21.0554
0.2		15.6489	15.6595	15.6592
0.3		10.0894	10.0888	10.0750
0.1	He, $(1s3p)^3P$	33.2233	33.1520	33.0946
0.2		20.2710	20.3149	20.1579
0.3		10.2145	10.2350	10.2863
0.1	He, $(1s4p)^3P$	39.8836	41.9651	42.0424
0.2		20.9864	20.2383	20.0781
0.3		8.1456	7.9045	7.9585
0.1	Li <sup>+</sup> , $(1s2p)^3P$	5.7974	5.5209	5.5216
0.2		5.3458	5.0908	5.0912
0.3		4.6884	4.4644	4.4644
0.1	He, $(1s2p)^1P$	17.4475	17.4809	17.4710
0.2		12.3005	12.2962	12.3033
0.3		7.3245	7.3024	7.3065
0.1	He, $(1s3p)^1P$	30.4172	30.5785	30.6182
0.2		17.4416	17.3700	17.1937
0.3		7.9201	7.8680	7.8831
0.1	He, $(1s4p)^1P$	40.0922	41.0226	40.8137
0.2		18.4176	17.8297	17.5213
0.3		6.2366	6.2375	6.3933
0.1	Li <sup>+</sup> , $(1s2p)^1P$	4.7574	4.7614	4.7628
0.2		4.3336	4.3371	4.3381
0.3		3.7301	3.7325	3.7330

are larger for the excited states for the first few values of the photoelectron momentum.

In Tables IX and X, the photoionization cross sections are presented for Li<sup>+</sup>. They are much smaller compared to the cross sections for He. Table IX shows that the  $(1s2p)$  and  $(1s3p)$  triplet states of the Li ion have a minimum in  $\sigma(l_f = 0)$ .

Jacobs [20] calculated the photoionization of the  $(1s2p)^1P$  state of a helium atom by using the close-coupling approximation. His results (obtained by multiplying the partial oscillator strengths by  $4\pi^2\alpha a_0^2 = 8.062$  Mb) are compared with the present results in Table XI, and the close-coupling results are seen to be lower than the present results. This comparison is also shown in Fig. 1.

Gisselbrecht *et al.* [21] have carried measurements of the photoionization cross sections of the  $(1s2p)^1P$  and  $(1s3p)^1P$  states of a helium atom by using picosecond tunable lasers. Their measured cross sections for the  $(1s2p)^1P$  state for the photoelectron momenta of 0.094 and 0.308 are 16.6 and 6.6 Mb, respectively, while the present results at 0.10 and 0.30 are 17.74 and 7.44 Mb, respectively. The agreement is fairly good considering that the accuracy of the measurements is 25%. A similar measurement of the  $(1s3p)^1P$  state at the photoelectron momenta of 0.105, 0.247, and 0.382 are 24.4, 10.5, and 4.2 Mb, while the inferred present results from interpolation are 30.28, 12.68, and 4.39 Mb, respectively. Again the agreement is fairly good considering the accuracy of 25% of the measurements.

A similar experiment on the  $(1s3p)^1P$  state of He has been carried out by Haber *et al.* [22] at exactly the same

TABLE VII. Total photoabsorption cross sections (Mb) for <sup>3</sup>P states of He.

<i>k</i>	(1s2p) <sup>3</sup> P state of He		
	<i>l<sub>f</sub></i> = 0	<i>l<sub>f</sub></i> = 2	Total
0.1	2.3910(-1)	21.0554	23.4464
0.2	1.8014(-1)	15.6592	15.8393
0.3	1.1695(-1)	10.0750	10.1920
0.4	6.8129(-2)	5.9141	5.9822
0.5	3.6952(-2)	3.3080	3.3450
0.6	1.8835(-2)	1.8176	1.8364
0.7	9.2323(-3)	9.9685(-1)	1.0061
0.8	4.3557(-3)	5.5048(-1)	5.5484(-1)
0.9	2.0342(-3)	3.0629(-1)	3.0832(-1)
1.0	9.4772(-4)	1.7121(-1)	1.7216(-1)
1.1	4.8002(-4)	9.5712(-2)	9.6192(-2)
1.2	2.6010(-4)	5.2213(-2)	5.2473(-2)
1.3	1.9561(-4)	2.7001(-2)	2.7021(-2)
1.4	2.3343(-4)	1.3331(-2)	1.3564(-2)
1.5	1.8114(-4)	5.8450(-3)	6.0261(-3)
1.6	2.2273(-4)	2.0162(-3)	2.2435(-3)
1.7	2.7622(-4)	3.6277(-4)	6.3899(-4)
	(1s3p) <sup>3</sup> P state of He		
0.1	7.3841(-1)	33.0946	33.8330
0.2	4.3019(-1)	20.1579	20.5881
0.3	2.1182(-1)	10.2863	10.4981
0.4	1.0031(-1)	4.8458	4.9461
0.5	4.7466(-2)	2.2735	2.3210
0.6	2.2293(-2)	1.0978	1.1201
0.7	1.1184(-2)	5.4599(-1)	5.5717(-1)
0.8	5.8524(-3)	2.7979(-1)	2.8564(-1)
0.9	3.0489(-3)	1.4697(-1)	1.5002(-1)
1.0	1.6386(-3)	7.9557(-2)	8.1196(-2)
1.1	8.6149(-4)	4.3627(-2)	4.4488(-2)
1.2	4.2846(-4)	2.3857(-2)	2.8142(-2)
1.3	2.6229(-4)	1.2919(-2)	1.3181(-2)
1.4	1.2897(-4)	6.5604(-3)	6.6894(-3)
1.5	7.1650(-5)	3.0872(-3)	3.1589(-3)
1.6	3.6230(-5)	1.2820(-3)	1.3182(-3)
1.7	1.4598(-5)	3.9579(-4)	4.1039(-4)
	(1s4p) <sup>3</sup> P state of He		
0.1	1.3997	42.0424	43.4421
0.2	6.0959(-1)	20.0781	20.6877
0.3	2.2155(-1)	7.9585	8.1801
0.4	9.0705(-2)	3.3211	3.4118
0.5	3.5954(-2)	1.3712	1.4072
0.6	1.4252(-2)	5.9616(-1)	6.1041(-1)
0.7	6.1057(-3)	2.8723(-1)	2.9334(-1)
0.8	2.8543(-3)	1.4558(-1)	1.4843(-1)
0.9	1.3618(-3)	7.5135(-2)	7.6497(-2)
1.0	6.3061(-4)	3.9231(-2)	3.9862(-2)
1.1	3.5675(-4)	2.0728(-2)	2.1085(-2)
1.2	1.5936(-4)	1.1067(-2)	1.1226(-2)
1.3	9.4393(-5)	5.8585(-3)	5.9794(-3)
1.4	7.4255(-5)	2.8313(-3)	2.9056(-3)
1.5	5.4261(-5)	1.4899(-3)	1.5442(-3)
1.6	5.6225(-5)	6.5995(-4)	7.1618(-4)
1.7	4.5292(-5)	2.3360(-4)	2.7889(-4)

TABLE VIII. Total photoabsorption cross sections (Mb) for <sup>1</sup>P states of He.

<i>k</i>	(1s2p) <sup>1</sup> P state of He		
	<i>l<sub>f</sub></i> = 0	<i>l<sub>f</sub></i> = 2	Total
0.1	2.6918(-1)	17.4710	17.7402
0.2	2.0605(-1)	12.3033	12.5094
0.3	1.3860(-1)	7.3065	7.4451
0.4	8.5132(-2)	3.9050	3.9901
0.5	4.9795(-2)	1.9759	2.0257
0.6	2.8560(-2)	9.7950(-1)	1.0081
0.7	1.6168(-2)	4.8812(-1)	5.0429(-1)
0.8	8.9870(-3)	2.4743(-1)	2.5642(-1)
0.9	5.0053(-3)	1.2916(-1)	1.3417(-1)
1.0	2.7539(-3)	6.9854(-2)	7.2608(-2)
1.1	1.5556(-3)	3.9702(-2)	4.1258(-2)
1.2	8.4475(-4)	2.3663(-2)	2.4508(-2)
1.3	4.5915(-4)	1.4296(-2)	1.5419(-2)
1.4	2.3343(-4)	9.3548(-3)	9.5882(-3)
1.5	1.0795(-4)	6.5929(-3)	6.7009(-3)
1.6	5.0196(-5)	4.9742(-3)	5.0244(-3)
1.7	2.1510(-5)	4.0039(-3)	4.0254(-3)
	(1s3p) <sup>1</sup> P state of He		
0.1	7.3841(-1)	30.6182	31.3566
0.2	4.3019(-1)	17.1937	17.6239
0.3	2.1182(-1)	7.8831	8.0949
0.4	1.0031(-1)	3.3590	3.4593
0.5	4.7466(-2)	1.4081	1.4556
0.6	2.2293(-2)	6.0690(-1)	6.2919(-1)
0.7	1.1184(-2)	2.7474(-1)	2.8592(-1)
0.8	5.8524(-3)	1.2836(-1)	1.3421(-1)
0.9	3.0489(-3)	6.2325(-2)	6.5374(-2)
1.0	1.6386(-3)	3.1757(-2)	3.3396(-2)
1.1	8.6149(-4)	1.7145(-2)	1.8006(-2)
1.2	4.2846(-4)	9.5360(-3)	9.9645(-3)
1.3	2.6229(-4)	5.4677(-3)	5.7300(-3)
1.4	1.2897(-4)	3.3547(-3)	3.4837(-3)
1.5	7.1650(-5)	2.4578(-3)	2.5295(-3)
1.6	3.6230(-5)	1.7689(-3)	1.8051(-3)
1.7	1.4598(-5)	1.3604(-3)	1.3750(-3)
	(1s4p) <sup>1</sup> P state of He		
0.1	1.2628	40.8137	42.0765
0.2	5.3909(-1)	17.5213	18.0604
0.3	2.0020(-1)	6.3933	6.5935
0.4	7.8501(-2)	2.3140	2.3925
0.5	3.1604(-2)	8.6143(-1)	8.9303(-1)
0.6	1.4261(-2)	3.4453(-1)	3.5879(-1)
0.7	6.4289(-3)	1.4763(-1)	1.5406(-1)
0.8	3.1733(-3)	6.7067(-2)	7.0240(-2)
0.9	1.6266(-3)	3.1810(-2)	3.3437(-2)
1.0	8.5656(-4)	1.5824(-2)	1.6681(-2)
1.1	4.3334(-4)	8.2951(-3)	8.7284(-3)
1.2	2.7873(-4)	4.4681(-3)	4.7468(-3)
1.3	1.3237(-4)	2.5827(-3)	2.7151(-3)
1.4	8.9883(-5)	1.6329(-3)	1.7228(-3)
1.5	3.5560(-5)	1.0909(-3)	1.1265(-3)
1.6	2.4817(-5)	7.7907(-4)	8.0389(-4)
1.7	2.7506(-5)	5.9654(-4)	6.2405(-4)

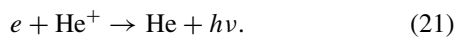
TABLE IX. Total photoabsorption cross sections (Mb) for  ${}^3P$  states of  $\text{Li}^+$ .

$k$	$(1s2p) {}^3P$ state of $\text{Li}^+$		
	$1_f = 0$	$1_f = 2$	Total
0.1	5.9179(-1)	5.5216	6.1134
0.2	5.4893(-1)	5.0912	5.6401
0.3	4.8548(-2)	4.4644	4.5129
0.4	4.0711(-2)	3.7444	3.7851
0.5	3.2391(-2)	3.0222	3.0546
0.6	2.4013(-2)	2.3644	2.3884
0.7	1.5771(-2)	1.8055	1.8213
0.8	7.8775(-3)	1.3524	1.3603
0.9	8.0765(-4)	9.9891(-1)	9.9972(-1)
1.0	2.4560(-2)	7.3009(-1)	7.5465(-1)
1.1	7.4757(-2)	5.2942(-1)	6.0418(-1)
1.2	7.8767(-2)	3.7994(-1)	4.5871(-1)
1.3	3.9808(-2)	2.7066(-1)	3.1047(-1)
1.4	2.6681(-2)	1.9367(-1)	2.2035(-1)
1.5	2.0021(-2)	1.3717(-1)	1.5719(-1)
1.6	1.6004(-2)	9.6423(-2)	1.1243(-1)
1.7	1.3321(-2)	6.7171(-2)	8.0492(-2)
$k$	$(1s3p) {}^3P$ state of $\text{Li}^+$		
	$1_f = 0$	$1_f = 2$	Total
0.1	1.9106(-1)	9.4797	9.6708
0.2	1.6524(-1)	8.2323	8.3975
0.3	1.3083(-1)	6.6135	6.7445
0.4	9.7003(-2)	4.9415	5.9115
0.5	6.8820(-2)	3.5349	3.6037
0.6	4.6509(-2)	2.4566	2.5017
0.7	3.0390(-2)	1.6792	1.7096
0.8	1.8446(-2)	1.1371	1.1555
0.9	8.3303(-3)	7.6663(-1)	7.7496(-1)
1.0	2.7700(-6)	5.1688(-1)	5.1689(-1)
1.1	1.5807(-1)	3.4944(-1)	5.0751(-1)
1.2	2.4139(-2)	2.3833(-1)	2.6247(-1)
1.3	1.3291(-2)	1.6048(-1)	1.7377(-1)
1.4	8.9921(-3)	1.1373(-1)	1.2272(-1)
1.5	6.6529(-3)	7.7210(-2)	8.3863(-2)
1.6	5.2192(-3)	5.3401(-2)	5.8620(-2)
1.7	4.1964(-2)	3.6857(-2)	4.1053(-2)

photoelectron momenta of 0.105, 0.247, and 0.382, and their corresponding results are  $24 \pm 6.1$ ,  $10.5 \pm 2.6$ , and  $4.2 \pm 1.1$  Mb. These measurements too have an error of 25%. A comparison of the results obtained in Ref. [21] with the presently obtained cross sections is shown in Fig. 2.

### III. RADIATIVE ATTACHMENT

As mentioned above, the radiative attachment or recombination process plays an important role in the solar and astrophysical problems. It is given by



The incident electron has angular momentum  $l = 0$  or 2 to give the He atom in the singlet or triplet  $(1s2p)$   $P$  state. Instead of  $\text{He}^+$ , the target can be  $\text{Li}^{2+}$ , giving  $\text{Li}^+$  in the final state. These processes are exothermal processes and have a small radiative-attachment cross section compared to the photoionization cross section  $\sigma$ . The attachment cross section

TABLE X. Total photoabsorption cross sections for  ${}^1P$  states of  $\text{Li}^+$ .

$k$	$(1s2p) {}^1P$ state of $\text{Li}^+$		
	$1_f = 0$	$1_f = 2$	Total
0.1	5.6034(-2)	4.7628	4.8188
0.2	5.2144(-2)	4.3381	4.3902
0.3	4.6482(-2)	3.7330	3.7795
0.4	3.9932(-2)	3.0571	3.0970
0.5	3.3022(-2)	2.3981	2.4311
0.6	2.6590(-2)	1.8192	1.8456
0.7	2.0950(-2)	1.3456	1.3666
0.8	1.6120(-2)	9.7814(-1)	9.9426(-1)
0.9	1.2312(-2)	7.0360(-1)	7.1591(-1)
1.0	9.3103(-3)	5.0376(-1)	5.1307(-1)
1.1	6.9730(-3)	3.6017(-1)	3.6714(-1)
1.2	5.2005(-3)	2.5624(-1)	2.6144(-1)
1.3	3.8745(-3)	1.8324(-1)	1.8711(-1)
1.4	2.8952(-3)	1.3353(-1)	1.3643(-1)
1.5	2.1322(-3)	9.7684(-2)	9.9812(-2)
1.6	1.5701(-3)	7.2468(-2)	7.4038(-2)
1.7	1.1636(-3)	5.4575(-2)	5.5739(-2)
$k$	$(1s3p) {}^1P$ state of $\text{Li}^+$		
	$1_f = 0$	$1_f = 2$	Total
0.1	1.7369(-1)	8.9895	9.1632
0.2	1.5008(-1)	7.6618	7.8119
0.3	1.1892(-1)	5.9729	6.0918
0.4	8.7412(-2)	4.2978	4.3852
0.5	6.1976(-2)	2.9515	3.0135
0.6	4.2760(-2)	1.9677	2.0105
0.7	2.8983(-2)	1.2920	1.3210
0.8	1.9773(-2)	8.4215(-1)	8.6192(-1)
0.9	1.3509(-2)	5.4763(-1)	5.6114(-1)
1.0	9.2442(-3)	3.5740(-1)	3.6664(-1)
1.1	6.2466(-3)	2.3496(-1)	2.4121(-1)
1.2	4.3094(-3)	1.5808(-1)	1.6239(-1)
1.3	3.0363(-3)	1.0470(-1)	1.0774(-1)
1.4	2.1247(-3)	7.2697(-2)	7.4822(-2)
1.5	1.5030(-3)	5.0774(-2)	5.2277(-2)
1.6	1.0603(-3)	3.5855(-2)	3.6915(-2)
1.7	7.6716(-4)	2.5779(-2)	2.6546(-2)

TABLE XI. Comparison of the present results of photoionization of the  $(1s2p) {}^1P$  state of He with those of Jacobs [20].

$k$	$\sigma(1_f = 0) + \sigma(1_f = 2)$	Jacobs [20] <sup>a</sup>
0.4	3.9901	2.7304
0.5	2.0257	1.4000
0.6	1.0081	7.2083(-1)
0.7	5.0429(-1)	3.6214(-1)
0.8	2.5642(-1)	1.7616(-1)
0.9	1.3417(-1)	8.4919(-2)
1.0	7.2608(-2)	4.2709(-2)
1.1	4.1258(-2)	3.2429(-2)
1.2	2.4508(-2)	1.0646(-2)
1.3	1.5419(-2)	6.4050(-2)

<sup>a</sup>Interpolated.

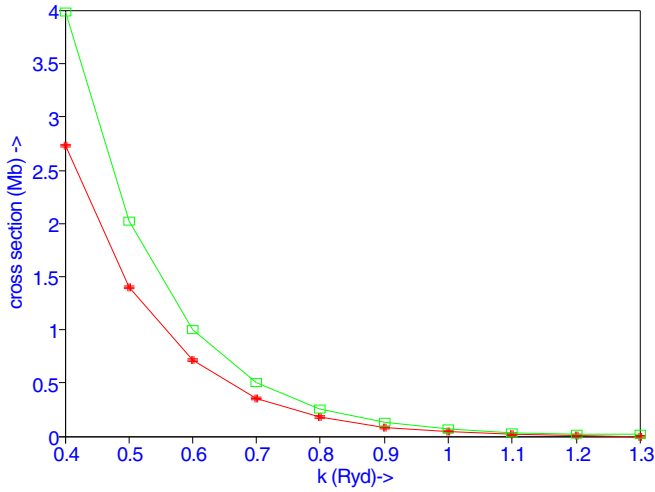


FIG. 1. (Color online) The upper curve represents photoionization cross sections of the  $(1s2p) \ ^1P$  state of the helium atom obtained in the present calculation, while the lower curve represents results obtained by Jacobs [20], using the close-coupling approximation.

is given by

$$\sigma_a = \left(\frac{h\nu}{cp_e}\right)^2 \frac{g(f)}{g(i)} \sigma = \left(\frac{h\nu}{c}\right)^2 \frac{1}{2mE} \frac{g(f)}{g(i)} \sigma, \quad (22)$$

which follows from the principle of detailed balance. In the above equation,  $p_e \equiv k$  is the electron momentum. The radiative rate coefficient averaged over the Maxwellian velocity distribution  $f(E)$  is given by

$$\alpha_R(T) = \langle \sigma_a v_e f(E) \rangle, \quad (23)$$

where  $v_e$  is the electron velocity, and the rate coefficient is given by

$$\alpha_R(T) = \sqrt{2/\pi} \frac{c}{(mc^2 k_B T)^{1.5}} \frac{g(f)}{g(i)} \int_0^\infty dE (E+I)^2 \sigma e^{-E/k_B T}, \quad (24)$$

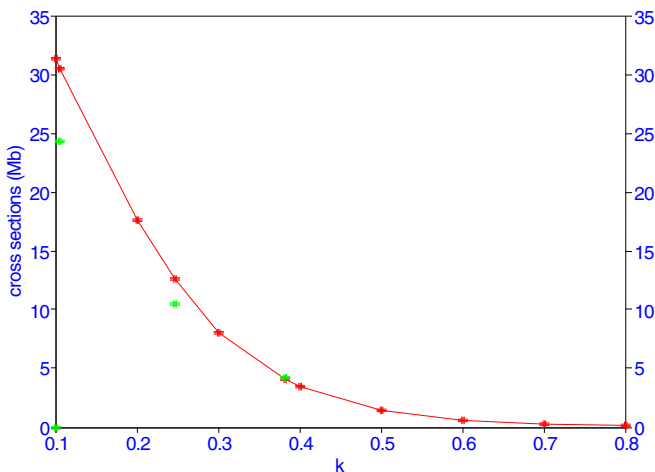


FIG. 2. (Color online) The solid curve represents photoionization cross sections of the  $(1s3p) \ ^1P$  state of the helium atom, while points represent the cross sections obtained in Ref. [21]. These measurements have an accuracy of 25%.

TABLE XII. Recombination rate coefficients ( $\text{cm}^3/\text{s}$ ) for the  $3,1P$  states of He and  $\text{Li}^+$ .

$T$ (K)	$10^{15} \alpha_R$ (T)			
	He( $^3P$ )	He( $^1P$ )	Li $^+$ ( $^3P$ )	Li $^+$ ( $^1P$ )
1000	31.54	7.73	178.96	31.04
2000	29.62	7.21	169.79	29.45
5000	21.76	5.19	123.94	22.38
7000	18.68	4.41	104.78	19.58
10 000	15.53	3.61	85.74	16.70
12 000	14.01	3.23	76.88	15.30
15 000	12.24	2.79	66.95	13.60
17 000	11.30	2.56	61.85	12.78
20 000	10.15	2.28	55.69	11.69
22 000	9.51	2.12	52.32	11.07
25 000	8.68	1.92	48.07	10.28
30 000	7.59	1.66	42.54	9.21
35 000	6.74	1.46	38.30	8.37
40 000	6.05	1.30	34.95	7.68

where  $E = k^2$  is the energy of the electron,  $k_B$  is the Boltzmann constant,  $T$  is the electron temperature, and  $h\nu = E + I$ , where  $I$  is the threshold for photoionization. Considering the spin states of the electron, the angular momentum, and the

TABLE XIII.  $P$ -state energies of He and  $\text{Li}^+$  for various numbers of terms.

System	State	$a$	$B$	$N_\omega$	$E$ (Ry)
He	$(1s2p) \ ^3P$	0.91	2.25	220	-4.266 328 36
		0.91	2.30	286	-4.266 328 37
		0.91	2.30	364	-4.266 328 38
He	$(1s3p) \ ^3P$	0.56	1.91	220	-4.116 161 96
		0.56	1.91	286	-4.116 162 04
		0.56	1.91	364	-4.116 162 11
He	$(1s2p) \ ^3P$	0.41	1.97	220	-4.064 645 74
		0.43	1.93	286	-4.064 648 19
		0.43	1.93	364	-4.064 648 19
He	$(1s2p) \ ^1P$	0.86	2.08	220	-4.247 686 12
		0.86	2.08	286	-4.247 686 15
		0.86	2.08	364	-4.247 686 16
He	$(1s3p) \ ^1P$	0.57	2.01	220	-4.110 292 25
		0.58	2.13	286	-4.110 292 51
		0.58	2.13	364	-4.110 292 63
He	$(1s4p) \ ^1P$	0.40	1.95	220	-4.062 136 34
		0.41	2.04	286	-4.062 138 07
		0.41	2.04	364	-4.062 138 66
Li $^+$	$(1s2p) \ ^3P$	1.70	3.55	220	-10.055 431 4
		1.74	3.57	286	-10.055 431 4
		1.74	3.57	364	-10.055 431 4
	$(1s3p) \ ^3P$	1.08	3.02	220	-9.460 919 2
		1.11	3.02	286	-9.460 919 3
		1.16	3.02	364	-9.460 919 3
	$(1s2p) \ ^1P$	1.70	3.45	220	-9.986 702 1
		1.80	3.15	286	-9.986 702 1
		1.85	3.45	364	-9.986 702 1
1.05		3.25	220	-9.440 133 1	
1.10		3.30	286	-9.440 136 0	
1.15		3.35	364	-9.440 137 1	

polarization directions of the electromagnetic field, we have  $g(i) = 4(2l_i + 1)$ , where  $l_i = 0$  or  $2$ , and  $g(f) = 6(2S + 1)$ , where  $S$  is the spin of the final state of the combined ion. The above expression can be written as

$$\alpha_R(T) = g(f)20.50169 \times 10^{10} \int_0^\infty dE(E+I)^2 \times \Sigma(E)e^{-E/k_B T}, \quad (25)$$

where

$$\Sigma(E) = [\sigma(E)/g(i)]_{l_i=0} + [\sigma(E)/g(i)]_{l_i=2}. \quad (26)$$

The photoionization cross section in Eq. (25) is in units of Mb. The rate coefficients, obtained using the photoionization cross section given in Tables VII–X for He and  $\text{Li}^+$ , are given in Table XII when the final state is a triplet or singlet  $P$  state. Very few energy points in Eq. (25) are required to get converged results. The rate coefficients for the higher excited states can be calculated easily using the cross sections given above. The rate coefficients are much larger in  $\text{Li}^+$  than in He and in all cases and they decrease with the increase of the electron temperature.

#### IV. CONCLUSIONS

The long-range potential has been included in the scattering equation variationally and therefore the present results for the phase shifts have lower bounds to the exact phase shifts. The present approach is applied to calculate photoionization

cross sections of singlet and triplet  $P$  excited states of He and  $\text{Li}^+$ . The present results are compared to those obtained using the close-coupling approximation [20] and the experimental results obtained using the tunable lasers [21,22]. There are very few measurements and the accuracy is not very good, and it is hoped that the present calculation will encourage new measurements and that the photoionization cross sections calculated here for various excited states will be useful in the investigation of solar and stellar objects. These cross sections are used here to calculate the Maxwellian-averaged radiative-attachment cross sections at various electron temperatures, the recombined states being  $^{1,3}P$  states of He and  $\text{Li}^+$ .

As for the accuracy of the calculations, all phase shifts and cross sections have converged to better than the third decimal place.

#### ACKNOWLEDGMENTS

Thanks are extended to Dr. R. J. Drachman for helpful comments.

#### APPENDIX

In Table XIII, we give the nonlinear parameters of various excited  $P$ -state energies of a He atom and a  $\text{Li}^+$  ion for a number of terms in the Hylleraas function, Eq. (13). All energies have converged to six or seven decimal places when the number of terms is increased from 220 to 286 and then to 364.

- 
- [1] C. Sinha and A. K. Bhatia, *Phys. Rev. A* **83**, 063417 (2011).
  - [2] A. K. Bhatia and C. Sinha, *Phys. Rev. A* **86**, 053421 (2012).
  - [3] A. Temkin, *Phys. Rev.* **107**, 1004 (1957).
  - [4] A. Temkin and J. C. Lamkin, *Phys. Rev.* **121**, 788 (1961).
  - [5] E. McGreevy and A. L. Stewart, *J. Phys. B* **10**, L527 (1977).
  - [6] D. H. Oza, *Phys. Rev. A* **33**, 824 (1986).
  - [7] T. Scholz, P. Scott, and P. G. Burke, *J. Phys. B* **21**, L139 (1988).
  - [8] J. Botero and J. Shertzer, *Phys. Rev. A* **46**, R1155 (1992).
  - [9] I. H. Sloan, *Proc. R. Soc. London, Ser. A* **281**, 151 (1964).
  - [10] P. Khan, M. Daskhan, A. S. Ghosh, and C. Falcon, *Phys. Rev. A* **26**, 1401 (1982).
  - [11] T. T. Gien, *J. Phys. B* **35**, 4475 (2002).
  - [12] T. T. Gien, *J. Phys. B* **36**, 2291 (2003).
  - [13] A. K. Bhatia, *Phys. Rev. A* **75**, 032713 (2007).
  - [14] A. K. Bhatia, *Phys. Rev. A* **77**, 052707 (2008).
  - [15] A. K. Bhatia, *Phys. Rev. A* **85**, 052708 (2012).
  - [16] A. K. Bhatia, *Phys. Rev. A* **86**, 032709 (2012).
  - [17] A. K. Bhatia, *Phys. Rev. A* **87**, 042705 (2013).
  - [18] K. Omidvar, *Phys. Rev.* **133**, A970 (1964).
  - [19] A. K. Bhatia and A. Temkin, *Rev. Mod. Phys.* **36**, 1050 (1964).
  - [20] V. L. Jacobs, *Phys. Rev. A* **9**, 1938 (1974).
  - [21] M. Gisselbrecht, D. Descamps, C. Lyngå, A. L'Huillier, C.-G. Wahlström, and M. Meyer, *Phys. Rev. Lett.* **82**, 4607 (1999).
  - [22] L. H. Haber, B. Doughty, and S. R. Leone, *Phys. Rev. A* **79**, 031401(R) (2009).